A novel method for detecting the fovea in fundus images of the eye

Pedro de Moura Garcia, Diego Luis Kreutz
Universidade Federal do Pampa (UNIPAMPA)
Alegrete, Rio Grande do Sul, Brasil
Email: pedrogarcia@alunos.unipampa.edu.br ;
diegokreutz@unipampa.edu.br

Daniel Welfer
Departamento de Computacao Aplicada - DCOM
Universidade Federal de Santa Maria (UFSM)
Santa Maria, Rio Grande do Sul, Brasil
Email: daniel.welfer@ufsm.br

***Abstract*—In this paper we propose a novel method for finding the fovea in colored images of the eye fundus. We use an image correlation coefficient to find the fovea, which is calculated from a set of template images of the fovea. The results, using the DIARETDB1 database, indicate that our method detects the fovea region with an accuracy of 82,02%.**

***Keywords*-fovea; image processing; cross-correlation; Diabetic retinopathy;**

I. Introduction

Diabetes is a widely spread chronic disease. The two main root causes of Diabetes are the insufficient production of insulin or the body's incapability of assimilating the produced insulin. In 2012, Diabetes was the direct cause of 1.5 million deaths around the world. More than 80% of those deaths happened in poor countries. According to the World Health Organization, nearly 9% of the world's population over 18 years had some form of Diabetes by 2014 [1].

Diabetes mellitus is a metabolic disorder that occurs either when the pancreas does not produce enough insulin or when the body cannot effectively use the insulin it produces. The effects of Diabetes include failure, dysfunction and damage to different organs in the long term. The World Health Organization classifies complications caused by Diabetes in macro vascular and micro vascular. Micro vascular complications are characterized as damages to small blood vessels, which can lead to blindness and kidney failure.

Diabetic retinopathy is a micro vascular complication of Diabetes resulted from the damages of small blood vessels in the back layer of the eye, which is also known as the retina. This complication leads to progressive loss of vision and can lead to blindness. The probability of developing Diabetic retinopathy increases with the time a person has Diabetes. The most effective way of diagnosing this disease is through regular eye examinations to identify early changes in the retina's blood vessels.

The Diabetic retinopathy lesions within the region of the macula, close or slightly away from the region of the fovea, have higher weights than other lesions. The automatic identification of the fovea center allows to qualify some lesions present on the fundus images (e.g., Diabetic macular edema lesions).

The fovea is responsible for the vision. It is essential to any activity that requires a high level of visual details. The fovea usually appears as a dark region on images of the fundus eye due to the absence of blood vessels. However, the presence of pathologies or inadequate lighting can change this feature on the captured images [2] [3].

The structure of the fovea has pixel intensity characteristics similar to other structures such as micro hemorrhages and micro aneurysms. This similarity represents a challenge for finding the fovea. In fact, it remains still an open research problem to accurately and efficiently find the fovea. Fig. 1 is an image, from the DIARETDB1 database, of a fundus eye that contains signs of Diabetic retinopathy. The location of the fovea is represented by the blue circle.

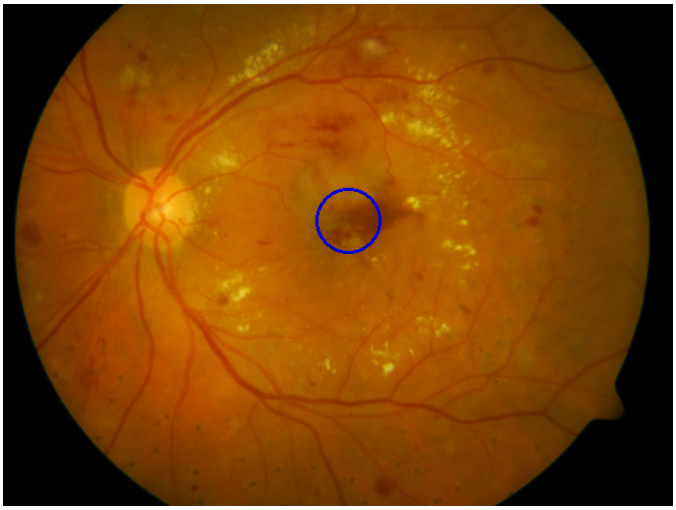

Fig. 1. A color eye fundus image from DIARETDB1 database

The diagnose of Diabetic retinopathy is commonly achieved by manually analyzing a large number of images. This is a costly and error-prone process. Tecnology can help to foster the development of automated tools for handling and analyzing large sets of images, reducing costs and leading to more accurate diagnoses. Previous research shows the need of automated procedures in order to improve the diagnoses process [4].

We propose a novel method for detecting the fovea using a visual approach. Unlike existing approaches, our method does not need to have any knowledge about other components of the eye, such as the optic disk or the blood vessels. We use a correlation coefficient and fovea templates extracted from real images.

We created a fovea template database from DIARETDB1's images. Each template has only one visibly identifiable component, the fovea. All colored images from the template and DIARETDB1 databases are converted to grayscale. After that, we use a normalized 2-D cross-correlation function to identify the fovea in the fundus image. The goal is to find the position of the maximum correlation between the template and the DIARETDB1 image.

The next step of our method is to calculate the average Euclidean distance between the positions of each template in relation to the others ones. The template that produces the smallest value of average Euclidean distance is chosen as the most probable location of the fovea. With this technique, we were able to find a valid location of the fovea in 73 of 89 images of the DIARETDB1 database.

II. Related work

The three approaches to detect fundus components, such as the fovea, are the visual, anatomical and the mixed. The first takes into account visual features of the image, such as color. The anatomical approach uses characteristics such as shape, location and distance from other fundus structures to detect specific components of the image. Finally, the last approach combines visual and anatomical aspects to locate the fovea. However, there is no winner among the different approaches regarding the accuracy to identify the fovea.

A. Visual approach

There are different methods using the visual approach. We are going to describe three of them. One using template images that mimic features of a fovea. A second method that uses contrast enhancements to detect the fovea and a third method combining five other methods to detect the center of the macula.

By mimiquim local features, the fovea can be located through a correlation function between the base image and fundus [5]. The criterion for the existence of the fovea is a correlation coefficient greater than 0.5. Additionally, other factors can also be used to locate the fovea, such as the acceptable distance from the optical disc and the darkest intensity area of the image.

Contrast enhancement on a fundus image allows the detection of the fovea by looking for the image structure with the lowest intensity [6]. In this method, the image structure with the lowest intensity is considered as the fovea.

More complex methods can be used to detect components such as the center of the macula [7]. One example is the combination of five different methods using the visual approach. The first step is to create a map with the partial results of each method. The results are analyzed taking into account different principles, which are combined to provide the final location of the center of the macula. The evaluation of the methods considered two criteria, the errors of the macula and the fovea. The error of the macula corresponds to the number of times the output of the algorithm fell within a established distance away from the macula center radius, selected manually. The Euclidean distance between the region of the fovea and the position of the ground truth is automatically identified, the ground truth was used to assess the accuracy of the method.

B. Anatomical approach

We introduce six methods based on the anatomical approach. The first detection method is based on the shape of the fovea combined with the location and positioning of the vascular arch, to restrict the searched area [2]. The course and direction of the blood vessels is identified using a template. The region of interest is defined by the identification of the blood vessels. The location of the fovea is obtained using a threshold scheme in the region of interest.

The second method is based on the fovea distance criterion and positioning of blood vessels [8]. First, the optical disc, and the arc vascular are located through a parabolic model. The position of the fovea is calculate using the location of these components.

The third method models the distribution of retinal components [9]. The molds of the structures are marked with different points on the image to identify the anatomy of the components. The settlement pattern is achieved when the pixel marked by the algorithm is at least 50 pixels away.

The fourth method uses thresholding and morphological techniques to find the fovea region [10]. The center of the optic disc and its surroundings are calculated using the Hough transform and morphological processing. A region of interest is defined through the spatial relationship between the fovea and the diameter of the optical disc. The center of the fovea is defined by the use of morphological operators and threshold applications.

The fifth method uses the blood vessels network of the retina to detect the fovea [11]. It is identified through the use of geometric techniques. This method is based on the fact that the fovea is located approximately 2.5 optical disc diameter in the temporal side of the optic nerve.

The sixth method removes the blood vessels from the image, and implements a multilimiar scheme along with an image smoothing to discover the fovea [12]. The center of the fovea is calculated on a contour map, created from the application of multilimiar scheme that uses grayscale values as criteria.

C. Mixed approach

There are different methods that use a mixed approach. We describe five of them.

The first method is designed to take into account low-resolution images [13]. The darkest pixel of the image is selected as a candidate of the fovea location in the original image. A circle is drawn using the darkest pixel as its center. The diameter of this circle is equal to twice the diameter of

the optical disc. While the darkest pixel represents the fovea, the circle around it represents the macula.

The second method finds the fovea through a model image and the position of the larger blood vessels contained in the retina [3]. A region of interest is established by the position of the optical disc and the blood vessels. A template image is used to detect the fovea in the region of interest using the correlation coefficient between the two images. The position of the fovea is defined where the correlation coefficient is higher.

The third method locates the center of the fovea through a region of interest [14]. This region of interest is established by calculating the distance between the fovea and the optical disk. The pixels representing the blood vessels are hidden through the use of morphological operations. The darker pixels are identified and grouped, the center of the fovea is identified as the most crowded position.

The fourth method uses concepts of mathematical morphology combined with anatomical knowledge to find the fovea center location [15]. The center and the diameter of the optic disc are calculated to define the region of interest where the fovea is located. A morphological processing is applied in order to obtain a set of candidate fovea. The central fovea is set as the candidate with the darkest region, located below an imaginary horizontal line, started from the center of the optical disc.

The fifth method consists in locating the center of the optical disc using the correlation between the template of an optical disk with the image [16]. A search for regions free of blood vessels is performed after the center of the optical disc is discovered. A line between the optical disc and the fovea is drawn. The fovea is detected using an adaptive Gaussian model for images with different resolutions by combining a mold around the fovea center axis of the previous step.

D. Discussion

Our method is based on the visual approach. It detects the fovea through the correlation between fundus images and real fovea templates. This is not implemented, nor evaluated, by any other method. The goal of using real fovea templates is to achieve a good accuracy and efficiency in detecting the fovea in fundus eye images showing lesions caused by diabetic retinopathy.

III. Technical Background

In this section we introduce some of the main concepts used in this work, such as the fundus, the Normalized 2-D cross-correlation, and the DIARETDB1 database.

A. Fundus

The fundus can be defined as the area within the eye that is located on the opposite side of the lens. Some of the structures found in the fundus are the retina, optic disc, macula, posterior pole and many blood vessels [17].

a) Optic disk: Is the entry point for the major blood vessels feeding the retina and also the start of the optic nerve. The same has very distinct characteristics of other components of the eye. In the fundus images, the optic disk is usually identified as the brightest region of the image, with a circular cut by blood vessels. The optic disk is represented by the circle located rightmost in Fig. 2. The location ranges from 3mm to 4mm for the nasal side of the fovea and has a central depression of variable size called optical cup [18] [3].

b) Macula: Is a rounded region located in the central area of the retina, typically having a diameter of approximately 5mm. In Fig. 2, the macula is represented as the largest circle located closer to the center of the image. The macula may be subdivided into lower layers, the outermost perifovea call and the intermediate parafovea. The innermost layer of the macula is known as the fovea [19] [20].

c) Fovea: Is responsible for sharp, central vision. Its importance is in the realization of activities that require a high level of visual detail, such as reading a text. The fovea is a small depression in the center of the retina of about 1 mm in diameter and located at a distance of about 2.5 times the diameter of the optical disc from it's center. It usually appears as a dark region on images of the fundus eye due to the absence of blood vessels. However, the presence of pathologies such as the Diabetic retinopathy, or inadequate lighting, can change this feature on the captured images. In Fig. 2, the fovea corresponds to the small dark circle in the center [12] [3] [2].

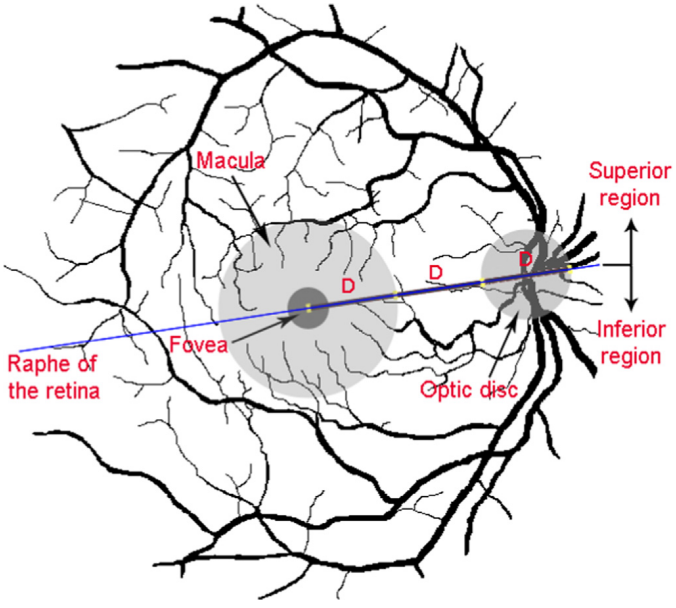

Fig. 2. A graphical representation of the eye fundus image according to Aquino [20]

B. Normalized 2-D cross-correlation

Cross-correlation is a standard method of estimating the degree to which two series are correlated. Images can be

first normalized for image-processing applications when the brightness of the image and template vary due to lighting and exposure conditions. This is typically done at every step by subtracting the mean and dividing by the standard deviation.

The normalized 2-D correlation between two images is calculated following these three steps [21]:

1 - Calculate the cross-correlation in the spatial or the frequency domain.

2 - Calculate local sums by precomputing running sums.

3 - Use local sums to normalize the cross-correlation to get correlation coefficients.

C. The DIARETDB1 database

DEARETDB1 is a database containing 89 colored images of the eye fundus. It contains 84 images with mild signs of non proliferative Diabetic retinopathy and 5 that can be considered as healthy. The images were captured at the Kuopio University Hospital with the same digital camera, always using an angle of 50 degrees, but with different settings like flash output, shutter speed, aperture and gain. The images have undergone a process of selection by medical specialists and the data is compatible with real cases found in hospitals. These images are appropriate to test and validate the performance for diagnostic methods [22].

IV. Fovea detection through correlation coefficients

We propose a method for detecting the fovea using the normalized 2-D cross-correlation between fundus images and fovea templates. Our method is described by the algorithm presented on Fig 3. The input images are the fovea templates database and the fundus image. These images are converted to grayscale. Each image corresponds to a matrix used as input in the normalized 2-D cross-correlation formula.

The normalized 2-D cross-correlation is represented by Formula 1. The input image is f, $\bar{t}$ is the mean of the template, and $\bar{f}_{u,v}$ is the mean of $f(x,y)$ in the region under the template. The output of Formula 1 is a new matrix that contains the correlation coefficients, which can range in value from -1.0 to 1.0. The value 1 represents a fully positive correlation, while 0 represents no correlation, and -1 is the completely negative correlation.

A new correlation matrix for each template is generated. The next step is to find the position of the maximum value in the correlation matrix for each template. To find the fovea, we calculate the Euclidean distance between each of the positions and the average Euclidean distance of each position to the center of the template. The template that has the lowest average distance is chosen as the most probable location of the fovea in the color eye fundus image. Next, a circle is drawn having as its center the coordinates of the central position of this template. This method aims to identify the fovea on healthy fundus images and also on those that present any lesions caused by some pathology.

Input: Fi = Fundus Image
Tdb = Fovea Templates database
t = Fovea Template
$Tdb = \{t_1, t_2, t_3, ...t_n\}$
1: Convert Fi and Tdb to Grayscale
2: **while** Tdb has n images **do**
3: NCC = Cross-correlation(t, Fi)
4: $[xt_n, yt_n]$ = position of NCC's max value
5: $Positions$ = $Positions$ $concat[xt_n, yt_n]$
6: **end while**
7: Calculate euclidean distance between all $Positions$
8: Calculate median distance for all $Positions$
9: $Plm =$ position with the lowest median
10: Out = Draw a circle from Plm on Fi
Output: Out {Final image}

Fig. 3. Fovea Detection Algorithm

$$\gamma(u,v) = \frac{\sum\limits_{x,y}[f(x,y) - \bar{f}_{u,v}][t(x-u,y-v) - \bar{t}]}{\{\sum\limits_{x,y}[f(x,y) - \bar{f}_{u,v}]^2 \sum\limits_{x,y}[t(x-u,y-v) - \bar{t}]^2\}^{0.5}} \quad (1)$$

V. Implementation

We created a fovea template database from DIARETDB1. Each fovea template represents the image of the fovea of a specific image from DIARETDB1. The fovea is extracted from each selected image, resulting in templates. Fig. 4 illustrates three templates used in the proposed method. They represent three different foveas, extracted from fundus images of the DIARETDB1.

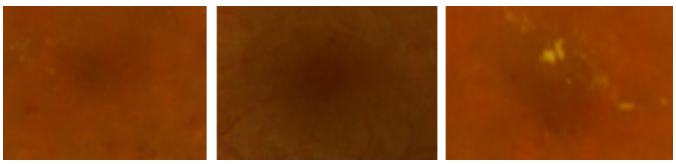

Fig. 4. Some templates used by the proposed method

As shown in Fig 3, the method gets as input the fundus image and the fovea template database. The fundus images from the DIARETDB1 and the images from the fovea template database are RGB images. As we used the normalized 2-D cross-correlation function, we had to convert all RGB images into two-dimensional grayscale images. Fig. 5 illustrates the conversion of an RGB eye fundus image to grayscale, as defined on line 1 of the algorithm shown in Fig 3. This conversion eliminates the information about the hue and saturation, while maintaining the luminance. The grayscale images correspond to different matrices, proportional to their sizes.

The second part of the proposed method is to correlate the fundus image with all images of the fovea template database,

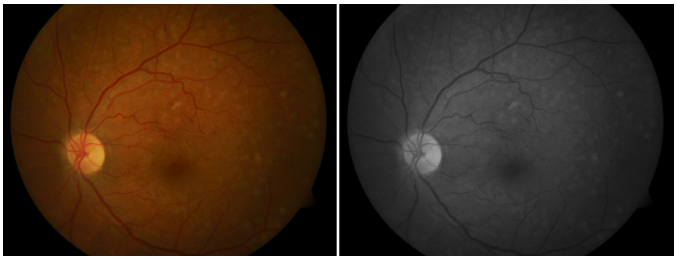

Fig. 5. Color eye fundus image converted into a grayscale image

as shown on line 3 of the algorithm shown in Fig 3. This correlation is calculated using the normalized 2-D cross-correlation. As a result, we have a new matrix for each fovea template.

Next, we find out the maximum correlation for each matrix (line 4, Fig 3). The maximum correlation value for each template is illustrated in Fig. 6. The position of maximum correlation corresponds to the center of each square.

The seventh line of the algorithm represents the calculation of the Euclidean distance between each of the maximum positions extracted from the resulting matrices. These distances are illustrated by the yellow lines in Fig. 7.

The average of the Euclidean distance is calculated for each of the positions, as shown in the eighth line of the algorithm. The template whose average produces the lowest value is chosen as the candidate of the possible localization of the fovea in the image. Lastly, a circle is drawn, having as its center the coordinates of the central position of this template (line 10 of the algorithm).

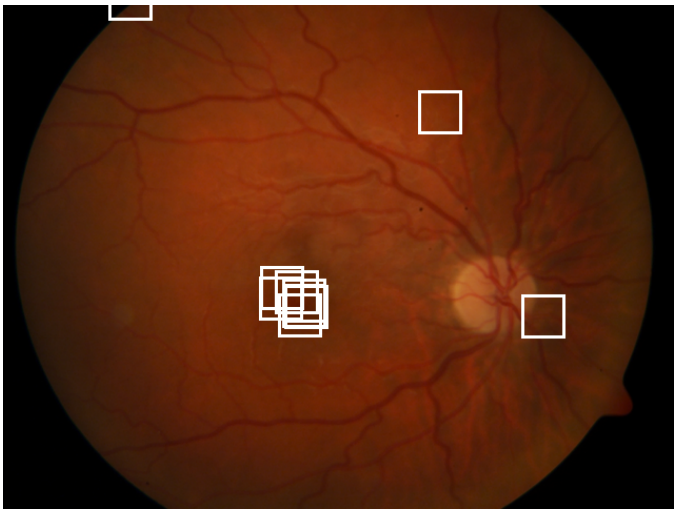

Fig. 6. The position of maximum correlation produced for each template of the proposed method

Our method has as output the original image of the fundus with a circle identifying the most probable location of the fovea. The center of this circle corresponds to the lowest average Euclidean distance between the positions of the templates. Fig. 8 and Fig. 9, illustrates an output of our method. In these images, the center of the blue circle represents the position with the maximum correlation to a given template. The centroid of this resulting circle is used as a reference point for the fovea center. It is worth emphasizing that, for clinical practice, only one result was achieved by image and this result is independent of a priori knowledge of the ground-truth.

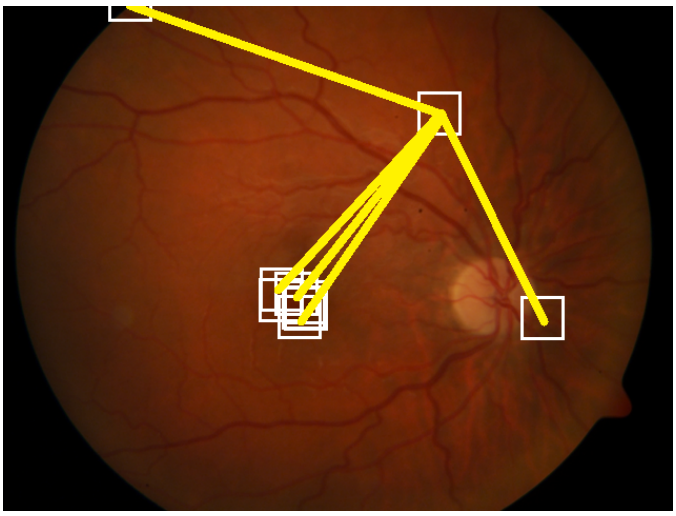

Fig. 7. Euclidean distance between the maximum positions obtained for each template

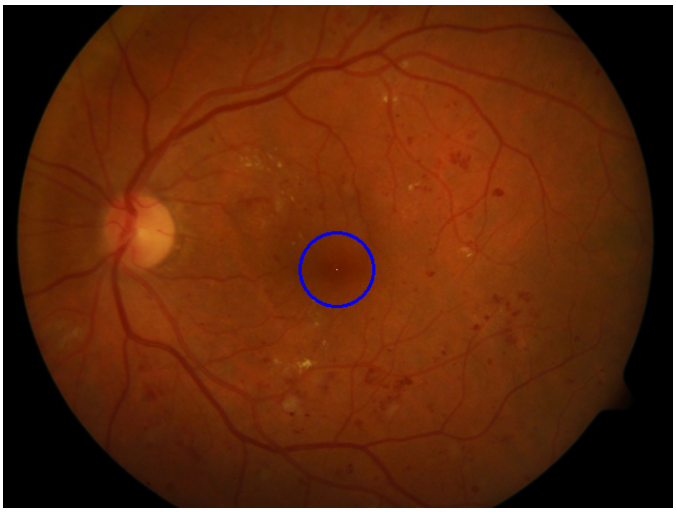

Fig. 8. Resulting image of the proposed method

VI. Results and Discussion

We created a fovea template database with 10 templates to evaluate our method. These ten images have different visual characteristics that help our method to find the fovea in a diversified set of fundus images. Table I shows the number of the original image from DIARETDB1 corresponding to each

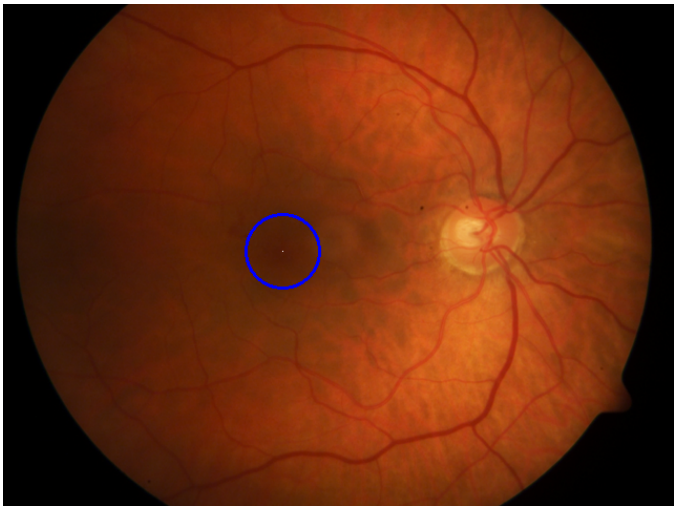

Fig. 9. Resulting image of the proposed method

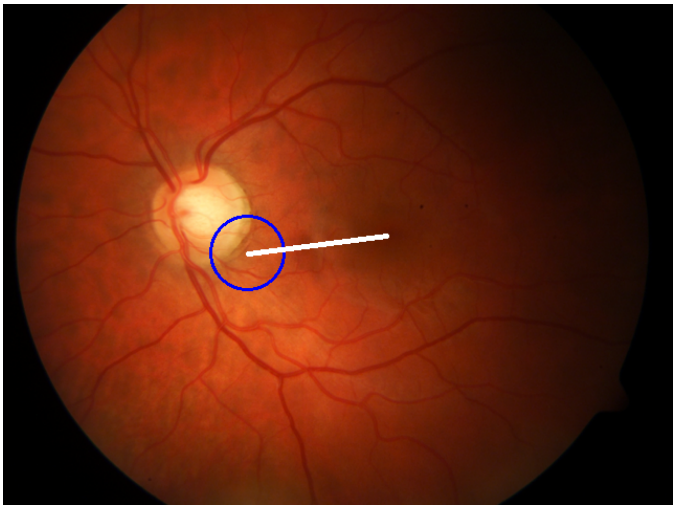

Fig. 10. Fovea that was incorrectly detected by the proposed method

TABLE I
FOVEA TEMPLATE DATABASE: ORIGINAL DIARETDB1 IMAGE OF EACH FOVEA TEMPLATE.

Template	DIARETDB1 Image
1	34
2	3
3	4
4	87
5	64
6	16
7	51
8	27
9	29
10	65

fovea template. We ran our experiments using this template database and all 89 images of DIARETDB1.

We used a ground truth provided by an expert on the field to evaluate the accuracy of our method. This ground truth is composed by 89 binary images, where the only existent white pixel corresponds to the center of the fovea. Each image of DIARETDB1 has a corresponding image with the ground truth.

To evaluate the location of the fovea, we use the same methodology proposed in [15]. We calculate the Euclidean distance between the position (x, y) that was found by the proposed method as the center of the fovea and the position established in the image of the ground truth. We considered as successful the results where the center of the fovea was found at a distance less than or equal to 40 pixels. In Table II and Table III we show the Euclidean distances for each image of the DIARETDB1 database. As you can observe, there are only a few failures on detecting the fovea.

Fig. 10 illustrates an example of an incorrectly detected fovea. The center of the blue circle is 136.06 pixels away from the ground truth of the fovea. While this is an extreme example of failure, our method achieved an average of 30.32 pixels of distance.

We also used the same validation process to identify the individual accuracy of the correlation templates. Table IV shows the results of each fovea template. The fovea templates that showed the best accuracy were #1 and #7. Both found a correct position of the fovea in 65 images. Followed by fovea templates #9 and #2, finding a valid position for 48 and 42 images, respectively. The templates #4 and #5 located the correct position of the fovea center in 32 and 26 images, respectively. The #10 was found in 14 images. Templates #6, #3 and #8 have produced the worst results since they found a valid position to the fovea in only 4, 3 and 2 images, respectively.

Although some templates have achieved a low success rate, we kept them in the template database. These templates were able to find some correct positions for the fovea on images where all others templates have failed. Therefore, it is importante to keep a good diversity of templates.

The main drawback of our approach is directly associated with some features of the selected templates. The templates with the lowest success rates have very particular visual features that are found only in a few images of DIARETDB1. Because of this lack of visual similarity, these templates have failed in the correct localization of the fovea in most images.

Table V shows a comparison of our method with the existing methods that used the DIARETDB1. Our method found a valid position of the fovea in 73 of the 89 DIARETDB1 images, which means a success rate of 82,02% using a visual approach. Qureshi et al. [7] achieved 98,74% success rate, also using a visual approach. Welfer et al. [15], and Kao et al. [16] used the mixed approach and achieved the same success rate of 92,13%.

Welfer et al. [15], Qureshi et al. [7], and Kao et al. [16] methods located the optic disk first, then they tried to find the fovea position. Although our method achieved a lower accuracy, it is the only one that does not need another eye fundus component to find the position of the fovea. This means that our approach is simpler than other known methods

TABLE II
FOVEA DETECTION ACCURACY OF OUR APPROACH USING THE EUCLIDEAN DISTANCE FOR EACH IMAGE OF THE DIARETDB1 DATABASE. IF THE EUCLIDEAN DISTANCE (ERROR) IS WITHIN 40 PIXELS, THEN THE FOVEA WAS SUCCESSFULLY DETECTED. OTHERWISE, THE FOVEA DETECTION FAILED.

Image	Distance in pixels	Evaluation
Image#1	5,09	Success
Image#2	9,05	Success
Image#3	65,27	Failure
Image#4	49,81	Failure
Image#5	27	Success
Image#6	7,28	Success
Image#7	144,25	Failure
Image#8	12,53	Success
Image#9	14,76	Success
Image#10	58,54	Failure
Image#11	1	Success
Image#12	23,4	Success
Image#13	14,86	Success
Image#14	8,94	Success
Image#15	68,94	Failure
Image#16	1,41	Success
Image#17	10	Success
Image#18	52,43	Failure
Image#19	136,52	Failure
Image#20	27,01	Success
Image#21	38,32	Success
Image#22	19,23	Success
Image#23	25,94	Success
Image#24	5	Success
Image#25	16,15	Success
Image#26	141,05	Failure
Image#27	147,36	Failure
Image#28	12,8	Success
Image#29	1,41	Success
Image#30	25,31	Success
Image#31	8,4	Success
Image#32	18,68	Success
Image#33	15,23	Success
Image#34	27,89	Success
Image#35	8,06	Success
Image#36	17,02	Success
Image#37	13	Success
Image#38	12,36	Success
Image#39	8,9	Success
Image#40	15,23	Success
Image#41	8,48	Success
Image#42	25,96	Success
Image#43	11,04	Success
Image#44	9,21	Success

proposed in the literature.

Sinthanayothin et al. [5] also used the correlation between a template and a fundus image to find the fovea. They achieved a success rate of 80,4% using an artificial template of the fovea. We achieved a success rate of 82,02% using ten models of the fovea. It is worth emphasizing that the templates were extracted from real eye fundus images. Although the two methods used different image databases, they have similar results using the correlation between templates and a fundus image database.

VII. CONCLUSION

Ophthalmology is an area still lacking automated solutions to increase the productivity and quality of daily tasks. There is room for the development of new methods and technologies

TABLE III
(CONTINUED) FOVEA DETECTION ACCURACY OF OUR APPROACH USING THE EUCLIDEAN DISTANCE FOR EACH IMAGE OF THE DIARETDB1 DATABASE. IF THE EUCLIDEAN DISTANCE (ERROR) IS WITHIN 40 PIXELS, THEN THE FOVEA WAS SUCCESSFULLY DETECTED. OTHERWISE, THE FOVEA DETECTION FAILED.

Image	Distance in pixels	Evaluation
Image#45	14,21	Success
Image#46	26,07	Success
Image#47	1	Success
Image#48	125,67	Failure
Image#49	136,066	Failure
Image#50	5	Success
Image#51	9,434	Success
Image#52	7,2	Success
Image#53	24,18	Success
Image#54	8,06	Success
Image#55	140,89	Failure
Image#56	15,81	Success
Image#57	9	Success
Image#58	1	Success
Image#59	7,8	Success
Image#60	4,47	Success
Image#61	11,18	Success
Image#62	13,08	Success
Image#63	38,27	Success
Image#64	28,79	Success
Image#65	116,29	Failure
Image#66	114,06	Failure
Image#67	4,47	Success
Image#68	7,81	Success
Image#69	36,68	Success
Image#70	11,04	Success
Image#71	40	Success
Image#72	137,93	Failure
Image#73	55,36	Failure
Image#74	8,94	Success
Image#75	6,08	Success
Image#76	7,07	Success
Image#77	4,12	Success
Image#78	11,04	Success
Image#79	12,36	Success
Image#80	15,23	Success
Image#81	2,23	Success
Image#82	15,62	Success
Image#83	6,32	Success
Image#84	13,41	Success
Image#85	21,37	Success
Image#86	8,5	Success
Image#87	21,37	Success
Image#88	10	Success
Image#89	14,31	Success

TABLE IV
SUCCESS RATE IN THE FOVEA LOCATION OBTAINED BY EACH TEMPLATE

Template	Correct Positions	Success Rate
#1	65	73,03%
#2	42	47,19%
#3	3	3,37%
#4	32	35,95%
#5	26	29,21%
#6	4	4,49%
#7	65	73,03%
#8	2	2,24%
#9	48	53,93%
#10	14	15,73%

TABLE V
COMPARISON WITH EXISTING METHODS.

Methods	Components	Approach	Success Rate
Welfer et al. [15]	Optic disk, Fovea	Mixed	92,13%
Qureshi et al. [7]	Optic disk, Fovea	Visual	98,74%
Kao et al. [16]	Optic disk, Fovea	Mixed	92,13%
Our method	Fovea	Visual	82,02%

capable of helping doctors and patients on the diagnosis and prevention of diseases.

In this paper, we proposed a new method based on correlation models to automatically identify the fovea center using color eye fundus images. We implemented a prototype and discussed the results comparing with existing methods.

Our method achieved a success rate of 82.02% in finding a valid position of the fovea for the images of the DIARETDB1 database. The method was able to detect the location of the fovea center in various situations, such as Diabetic lesions and uneven illumination.

As future work, we plan to improve the accuracy of the method. Although it found the correct position of the fovea in most images, the method also found incorrect positions for some images.

REFERENCES

[1] W. H. Organization, "Media centre, diabetes: Fact sheet number 312," January 2015. [Online]. Available: http://www.who.int/mediacentre/factsheets/fs312/en/

[2] H. Li and O. Chutatape, "Automated feature extraction in color retinal images by a model based approach," *IEEE Transactions on Biomedical Engineering*, vol. 51, no. 2, pp. 246–254, 2004. [Online]. Available: http://ieeexplore.ieee.org/stamp/stamp.jsp?arnumber=1262102

[3] A. D. Fleming, K. A. Goatman, S. Philip, J. A. Olson, and P. F. Sharp, "Automatic detection of retinal anatomy to assist diabetic retinopathy screening," *Physics in medicine and biology*, vol. 52, no. 2, p. 331, 2007.

[4] F. Laliberte, L. Gagnon, and Y. Sheng, "Registration and fusion of retinal images-an evaluation study," *IEEE Transactions on Medical Imaging*, vol. 22, no. 5, pp. 661–673, 2003. [Online]. Available: http://ieeexplore.ieee.org/stamp/stamp.jsp?arnumber=1207401

[5] C. Sinthanayothin, J. F. Boyce, H. L. Cook, and T. H. Williamson, "Automated localisation of the optic disc, fovea, and retinal blood vessels from digital colour fundus images," *British Journal of Ophthalmology*, vol. 83, no. 8, pp. 902–910, 1999.

[6] J. Singh, G. Joshi, and J. Sivaswamy, "Appearance-based object detection in colour retinal images," in *Image Processing, 2008. ICIP 2008. 15th IEEE International Conference on*, 2008, pp. 1432–1435. [Online]. Available: http://ieeexplore.ieee.org/stamp/stamp.jsp?arnumber=4712034

[7] R. J. Qureshi, L. Kovacs, B. Harangi, B. Nagy, T. Peto, and A. Hajdu, "Combining algorithms for automatic detection of optic disc and macula in fundus images," *Computer Vision and Image Understanding*, vol. 116, no. 1, pp. 138–145, 2012.

[8] K. W. Tobin, E. Chaum, V. Govindasamy, and T. Karnowski, "Detection of anatomic structures in human retinal imagery," *IEEE Transactions on Medical Imaging*, vol. 26, no. 12, pp. 1729–1739, 2007. [Online]. Available: http://ieeexplore.ieee.org/stamp/stamp.jsp?arnumber=4359034

[9] M. Niemeijer, M. Abramoff, and B. van Ginneken, "Segmentation of the optic disc, macula and vascular arch in fundus photographs," *IEEE Transactions on Medical Imaging*, vol. 26, no. 1, pp. 116–127, 2007. [Online]. Available: http://ieeexplore.ieee.org/stamp/stamp.jsp?arnumber=4039534

[10] S. Sekhar, W. Al-Nuaimy, and A. Nandi, "Automated localisation of optic disk and fovea in retinal fundus images," in *Signal Processing Conference, 2008 16th European*. IEEE, 2008, pp. 1–5.

[11] D. Santhi and D. Manimegalai, "An efficient approach to locate optic disc center, blood vessels and macula in retinal images," *Biomedical Engineering: Applications, Basis and Communications*, vol. 24, no. 05, pp. 425–434, 2012.

[12] M. E. Gegundez-Arias, D. Marin, J. M. Bravo, and A. Suero, "Locating the fovea center position in digital fundus images using thresholding and feature extraction techniques," *Computerized Medical Imaging and Graphics*, vol. 37, no. 5, pp. 386–393, 2013.

[13] L. Gagnon, M. Lalonde, M. Beaulieu, and M.-C. Boucher, "Procedure to detect anatomical structures in optical fundus images," in *Medical Imaging 2001*. International Society for Optics and Photonics, 2001, pp. 1218–1225.

[14] A. V. Sagar, S. Balasubramanian, and V. Chandrasekaran, "Automatic detection of anatomical structures in digital fundus retinal images." in *IAPR Conference on Machine Vision Applications*, 2007, pp. 483–486.

[15] D. Welfer, J. Scharcanski, and D. R. Marinho, "Fovea center detection based on the retina anatomy and mathematical morphology," *Computer methods and programs in biomedicine*, vol. 104, no. 3, pp. 397–409, 2011.

[16] E.-F. Kao, P.-C. Lin, M.-C. Chou, T.-S. Jaw, and G.-C. Liu, "Automated detection of fovea in fundus images based on vessel-free zone and adaptive gaussian template," *Computer methods and programs in biomedicine*, vol. 117, no. 2, pp. 92–103, 2014.

[17] B. Cassin and S. Solomon, "Dictionary of eye terminology," Gainesville, Florida: Triad Publishing Company,, 1990.

[18] W. Tasman and E. A. Jaeger, *Duane's Ophthalmology 2009 Edition*. Lippincott Williams and Wilkins, 2013.

[19] M. Yanoff, B. S. Fine, and B. S. Fine, *Ocular pathology*. Mosby/Elsevier, 2009.

[20] A. Aquino, "Establishing the macular grading grid by means of fovea centre detection using anatomical-based and visual-based features," *Computers in biology and medicine*, vol. 55, pp. 61–73, 2014.

[21] J. Lewis, "Fast normalized cross-correlation," in *Vision interface*, vol. 10, no. 1, 1995, pp. 120–123.

[22] T. Kauppi, V. Kalesnykiene, J.-K. Kamarainen, L. Lensu, I. Sorri, A. Raninen, R. Voutilainen, H. Uusitalo, H. Kälviäinen, and J. Pietilä, "The diaretdb1 diabetic retinopathy database and evaluation protocol." in *BMVC*, 2007, pp. 1–10.